energies

MDPI

Article

Evaluating the Potential of Multi-Anodes in Constructed Wetlands Coupled with Microbial Fuel Cells for Treating Wastewater and Bioelectricity Generation under High Organic Loads

Prashansa Tamta [1], Neetu Rani [1,*], Yamini Mittal [2,3] and Asheesh Kumar Yadav [2,3,4,*]

[1] University School of Environment Management, Guru Gobind Singh Indraprastha University, Dwarka 110078, New Delhi, India
[2] CSIR—Institute of Minerals and Materials Technology, Bhubaneswar 751013, Odisha, India
[3] Academy of Scientific and Innovative Research (AcSIR), Ghaziabad 201002, Uttar Pradesh, India
[4] Department of Chemical and Environmental Technology, Rey Juan Carlos University, 28933 Mostoles, Spain
* Correspondence: neetu_rani@ipu.ac.in (N.R.); asheesh.yadav@gmail.com (A.K.Y.)

Abstract: Multiple anodes can significantly enhance the treatment potential of constructed wetlands coupled with a microbial fuel cell (CW-MFC) system, which has not yet been explored. Thus, the present study evaluates the potential of multi-anodes and single cathode-based CW-MFC at significantly higher organic loading rates for treatment performance and bioelectricity generation. For this purpose, two identical but different materials, i.e., graphite granules (GG) and granular activated charcoal (GAC), were used to set up multiple anodes and single cathode-based CW-MFCs. The graphite granules (GG)-based system is named CW-MFC (GG), and the granular activated charcoal (GAC) based system is named as CW-MFC (GAC). These systems were evaluated for chemical oxygen demand (COD), NH_4^+-N removal efficiency, and electrical output at relatively higher organic loading rates of 890.11 g COD/m^3-d and 1781.32 g COD/m^3-d. At an OLR of 890.11 g COD/m^3-d, the treatment efficiency was found to be 24.8% more in CW-MFC (GAC) than CW-MFC (GG), whereas it was 22.73% more for CW-MFC (GAC) when OLR was increased to 1781.32 g COD/m^3-d. Whereas, NH_4^+-N removal efficiency was more in CW-MFC (GG) i.e., 56.29 ± 7% and 56.09 ± 3.9%, compared to CW-MFC (GAC) of 36.59 ± 3.8% and 50.59 ± 7% at OLR of 890.11 g COD/m^3-d and 1781.32 g COD/m^3-d, respectively. A maximum power density of 48.30 mW/m^3 and a current density of 375.67 mA/m^3 was produced for CW-MFC (GAC) under an organic loading rate of 890.11 g COD/m^3-d.

Keywords: multiple anode electrodes; wastewater treatment; bioelectricity generation; COD removal

Citation: Tamta, P.; Rani, N.; Mittal, Y.; Yadav, A.K. Evaluating the Potential of Multi-Anodes in Constructed Wetlands Coupled with Microbial Fuel Cells for Treating Wastewater and Bioelectricity Generation under High Organic Loads. *Energies* **2023**, *16*, 784. https://doi.org/10.3390/en16020784

Academic Editors: Booki Min and Md Tabish Noori

Received: 30 October 2022
Revised: 10 December 2022
Accepted: 29 December 2022
Published: 10 January 2023

1. Introduction

Efficient management and treatment of wastewater is one of the prime environmental challenges today. Although various traditional technologies are currently being used to deal with this challenge, there is a prerequisite to exploring more efficient processes to combat future needs. These conventional wastewater treatment technologies demand an ample amount of energy for their operation, along with a high level of operational complexity. Thus, a low-cost, self-sufficient, easily operable, and low-maintenance technology can be a promising solution. Constructed wetlands (CWs) are one of the conventional wastewater treatment technologies that is advantageous in terms of low-cost, ease of operation, least maintenance requirement; however, they have slow treatment processes due to strongly dominated anaerobic reactions and thus require a large land area for treating wastewater [1,2]. Meanwhile, bio-electrochemical systems such as microbial fuel cells (MFCs) have gained a lot of attention as wastewater treatment technology with simultaneous bioelectricity recovery as a by-product, but scaling up is the biggest challenge to incorporate into

the real world. To overcome these challenges through individual technologies, a novel integrated technology was introduced as the constructed wetland-integrated microbial fuel cell (CW-MFC) [3,4]. A typical CW-MFC consists of an MFC unit embedded into the traditional constructed wetland with a cathodic portion in the upper region in contact with atmospheric oxygen and an anodic portion in the deeper zone region, which is anaerobic by nature. However, in CW-MFCs, both the anodic and cathodic regions are made up of conductive material rather than non-conductive material (such as gravel) in the case of CWs. Organic matter is oxidized by both exo-electrogenic microbial activity and non-exo-electrogenic microbial activity, where exo-electrogenic microbial activity produces electrons and protons. These electrons are transferred to the anode by a redox shuttle, redox-active protein, or nanowire, and then reach the cathode via an external wire, while H^+ transfers to the cathode by means of diffusion [5–7]. The presence of conductive material functions as an electron acceptor in the bottom anaerobic region and thus enhances the process of organic matter oxidation compared to conventional CWs. Up to date, CW-MFC has been explored in several aspects, and its optimal performance depends on a number of parameters such as electrode type, size, material, position and spacing, microbial community, flow regime, hydraulic retention time, substrate, recirculation, internal resistance, etc. [8–12]. Among these, the electrode is one of the key parameters that significantly affects the treatment performance and electrical output of CW-MFCs. The ideal electrode material possesses characteristics such as good conductivity and microbial compatibility thus facilitating the attachment of microorganisms [13]. The electrode provides an enrichment site for electroactive bacteria to ease biofilm growth and control the electrochemical reactions. Electrode impacts on the functionality and efficiency of CW-MFC in terms of electrode material, number, size, type, packing, etc.; thus, selection of a suitable electrode material is a prerequisite for optimal performance of CW-MFCs. Electrode material and packing layers have an influence on the composition, richness, and diversity of microbes. Some researchers have shown that electrode material has a great impact on treatment performance and bioelectricity generation [7,14]. Generally, most of the CW-MFCs employ granular activated carbon and granular graphite as electrode materials owing to their strong chemical stability, low cost, suitable attachment site for electroactive bacteria, and good biocompatibility [7,15,16]. However, graphite and carbon materials are low-cost electrodes but less efficient compared to metal electrodes such as Pt, Mo, Ag, and Ti, which have a high cost [17]. To amplify treatment and power performance of electrodes, surface properties and conductivity are being modified [18,19]. However, these modifications are not very cost-effective and infuse complexity into the system. For instance, the anode electrode was modified with biochar-nZVI, which enhances the removal performance of polycyclic aromatic hydrocarbons (PAHs) in CW-MFCs, although the modification process is quite extensive [20]. Several researchers used composite electrodes in place of a single electrode, metal, or metal-free catalyst in their study owing to their low cost, higher efficiency, and increased active area [21–23].

The number of electrodes can also be a factor influencing pollutant removal and bioelectricity production. A multi-electrode system enhances the electrode surface area and facilitates the electron transfer process, which improves the performance of CW-MFC in terms of wastewater treatment and electricity generation. Multiple electrode systems can resolve one of the potential challenges in scaling up CW-MFC for its field-level application of decreased power output while increasing its volume because a single electrode is not enough for the maximum possible harvest of electrons available at the anode or dispensing electrons from the cathode to the oxidant (like oxygen) and protons [9,24]. However, very few studies have been conducted to understand the role of multi-electrodes in CW-MFC [25–27]. For example, a multiple biocathode CW-MFC system using three carbon-felt electrodes was investigated by Xu et al. [28] for a systematic evaluation of the relationship between N removal and electrical output and reported higher energy production and higher nitrogen removal. They reported that the maximum power density of the system increased from 12.56 mW/m^2 to 26.16 mW/m^2 when the biocathode number was changed

from 1 to 3 [9,29]. Further, Wang et al. [26] investigated a multi-anode tidal CW-MFC under a low inflow C/N ratio and characterized NO_3^--N and electricity-transforming bacteria. In another multi-anode system reported by Tang et al. [24], cathode conditions were investigated in parallel and combined connection modes of a 30 L CW-MFC for wastewater treatment and electrical output for an influent COD of 500 mg/L. Yang et al. [27] studied a two-anode and a single-cathode CW-MFC to understand long-term roles in power generation and treatment performance at a COD of 189.91 ± 14.45 mg/L. A multiple biocathode CW-MFC system using three carbon-felt electrodes was investigated by Xu et al. [28] for systematic evaluation of the relationship between N removal and electrical output and reported more energy production with higher nitrogen removal. However, these studies are conducted for comparatively lower organic loading rates. So, a multi-anode system's potential for higher organic loads is still unexplored.

Thus, the present study focuses on examining the potential of multiple electrode systems for treating significantly higher organic loading rates with two equally sized CW-MFCs, each consisting of four equally sized anodes (multiple electrode systems) and a cathode using granular graphite or activated charcoal as an electrode material under a high organic loading rate. Each anode was connected to the cathode with a separate external resistance in a parallel connection mode. Along with multiple anode microcosms, CW control microcosms were also experimented with and evaluated (supplementary file). The study for wastewater treatment performance and electrical performance was conducted under two different, significantly higher organic loading rates to examine the potential of multiple electrodes.

2. Materials and Methods

2.1. Wastewater Composition

Synthetic wastewater, which represents untreated household wastewater, was prepared using glucose as a carbon source. The composition of synthetic wastewater was adopted from literature and includes glucose (1 g/L and 2 g/L), $CaCl_2$ (0.0301 g/L), $MgCl_2.6H_2O$ (0.0371 g/L), KH_2PO_4 (0.0445 g/L), $(NH_4)_2SO_4$ (0.01119 g/L), $(NH_4)_2Fe(SO_4)_2.6H_2O$ (0.0842 g/L), and $NaHCO_3$ (0.0111 g/L). The trace element solution contains H_3BO_3 (0.15 g/L), $CaCl_2.6H_2O$ (0.15 g/L), $CuSO_4.5H_2O$ (0.03 g/L), $FeCl_3.6H_2O$ (1.5 g/L), $ZnSO_4.7H_2O$ (0.12 g/L), and KI (0.03 gm/L) 34.

2.2. Configuration

Two equally sized CW-MFCs were built using polyvinyl chloride pipes of 57 cm height and 11 cm diameter and named CW-MFC (GG) and CW-MFC (GAC), as shown in Figure 1a,b. The CW-MFC (GG) was fabricated using graphite granules of sizes 5–8 mm as electrode material, whereas another CW-MFC (GAC) was equipped with electrodes made up of activated charcoal granules of sizes 5–8 mm. The total working volume of each system was 2 L. Each CW-MFC microcosm consists of four anodes (anode 1 (A1), anode 2 (A2), anode 3 (A3), and anode 4 (A4)) and one cathode. In the bottom of PVC pipes, a 2 cm thick boulder (10–12 mm) layer was placed. Above this layer, a 5 cm-thick layer of granular graphite or activated charcoal was placed as anode 1 for the fabrication of CW-MFC (GG) and CW-MFC (GAC), respectively. This layer was separated with a 3 cm-thick layer made up of a double-layered perforated plastic liner and stone gravels 5–8 mm in size. Likewise, three more anodes were fabricated. The anodic and cathodic zones were separated with a double-layered plastic liner, glass wool, and stone gravels measuring 0.2–0.5 cm. Plastic liners were provided with 2–3 holes in them for proper passage of wastewater. Thereafter, a 5 cm layer of gravel was placed as a separator between the anodic and cathodic zones. Above this, a 19 cm-thick layer of granular graphite or activated charcoal granules is placed to act as a cathode. One graphite rod of 100 mm × 13 mm (length × width) was connected with an electrical wire is placed in each electrode as a charge collector or dispenser. All four anodic zones were provided with an anode sampling point from the anode, i.e., A1: 54 cm; A2: 46 cm; A3: 38 cm; and A4: 30 cm in both systems, whereas each microcosms cathode is

fitted with one effluent port at 7 cm from above. In both CW-MFC microcosms, all four anodes were separately connected to the cathode using an external resistance of 1 KΩ in a parallel manner.

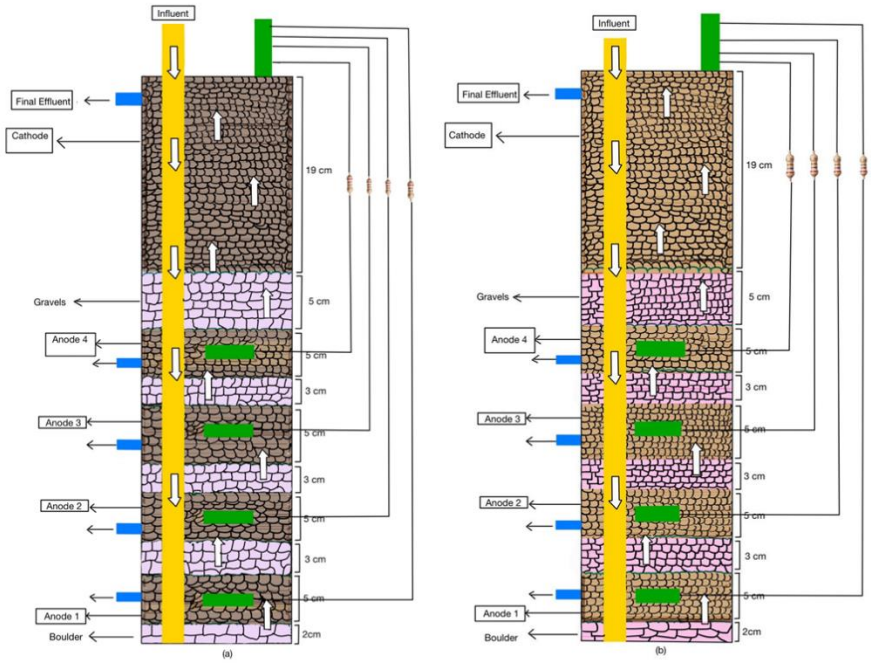

Figure 1. A schematic representation of configurations of (**a**) CW-MFC(GG) and (**b**) CW-MFC (GAC) setups used for the study.

2.3. Inoculation and Operation

CW-MFC(GG) and CW-MFC (GAC) were inoculated with a pre-acclimated microbial community of another CW-MFC, which had already been running for over a year in the CSIR-IMMT laboratory. After inoculation, each system was allowed to acclimatize for one and a half months before the start of the experiment. During this acclimatization phase, synthetic wastewater was regularly added to both CW-MFC microcosms in batch mode. After acclimatization, both microcosms were switched to continuous flow mode using a peristaltic pump at a flow rate of 1.16 mL/min. The wastewater was passed in an up-flow manner, from A1 upwards, eventually discharging from the cathode. The HRT for both microcosms was maintained for 24 h. Both systems were run at two organic loading rates. Initially, both systems were run, and all the experiments were conducted at an organic loading rate of 890.11 g COD/m^3-d. After that, the organic loading rate was changed to 1781.32 g COD/m^3-d. All the experiments were conducted at room temperature.

2.4. Measurement and Calculations

The water samples were collected through the outlet of each anodic sampling point for CW-MFC (GG) and CW-MFC (GAC). A 30 mL sample was taken from the outlet of each cell for chemical oxidation demand (COD) analysis. The COD was determined according to a standard method (APHA, 2005). Samples were taken from all four anodic and cathodic sampling points for dissolved oxygen (DO) and pH analysis. The measurements of pH were done using a pH meter (Eutech Instruments, Paisley, UK, CyberScan, pH 1500). The DO and NH_4^+-N measurements of the effluent were done using a portable multimeter (HACH HQ40D) with respective probes and reagents for each parameter. The percentage removal of COD and NH_4^+-N was calculated through the following Equation (1):

$$\%\ removal\ = \frac{influent\ concentration\ \left(\frac{mg}{L}\right) - effluent\ concentration\ \left(\frac{mg}{L}\right)}{influent\ concentration\ \left(\frac{mg}{L}\right)} \quad (1)$$

The voltage (V) was measured on a daily basis using a digital multimeter (Sanwa CD772) for CW-MFC (GG) and CW-MFC (GAC). Once voltage achieves the steady state, polarization study was carrying out by varying external resistance from 90 MΩ to 1 Ω and measuring voltage in every 20 min of interval. The electrical parameters were calculated by applying their standard formulas. Current (I) was calculated using Ohm's law, $I = V/R_{ex,}$ and power (W) were calculated using the standard formula, P = I.V where I is the current (A), V is the voltage (V in mV), and R_{ex} is the external resistance (Ω) across the electrodes. The volumetric power density (P_d) for each system was calculated using the formula $P_d = V^2/v.R_{ex}$ [30], where P_d is the volumetric power density (W/m^3) and v is the anodic volume (m^3). The current density of each system was calculated by dividing the current generated by the effective volume of each anodic zone of both CW-MFC microcosms. Thereafter, a polarization curve was plotted between current density, power density, and voltage to acquire the internal resistance of the system along with ohmic, concentration, and activation losses.

3. Results and Discussion

3.1. Environmental Conditions of Microcosms

Dissolved oxygen (DO) is one of the crucial factors that play a key role in the performance of CW-MFC. The dissolved oxygen concentrations (mg/L) observed during the course of study for CW-MFC (GG) and CW-MFC (GAC) are depicted in Figure 2a,b. In CW-MFC (GG), the DO concentrations were observed in the range of 1.09 ± 0.05 mg/L to 1.43 ± 0.07 mg/L from A1 to cathode at an organic loading rate of 890.11 g COD/m^3-d. Similarly, in CW-MFC (GAC), it ranged from 0.75 ± 0.06 to 1.78 ± 0.1 mg/L from A1 to the cathode. For an organic loading rate of 1781.32 g COD/m^3-d, DO levels were ranged from 0.96 ± 0.1 mg/L to 1.94 ± 0.07 mg/L from A1 to the cathode in CW-MFC (GG) whereas for CW-MFC (GAC), it ranged from 0.35 ± 0.04 mg/L to 3.28 ± 0.3 mg/L starting from A1 to the cathode. The DO levels significantly vary across both up-flow CW-MFCs. For both organic loading rates, the DO levels were found higher in the cathodic zone as compared to the anodic zone in CW-MFC (GG) as well as in CW-MFC (GAC). This can be attributed to the diffusion of air into the cathodic zone from the atmosphere, and since wastewater has a low organic matter content as it flows upward from the anodic zone to the cathodic zone, it no longer consumes the DO present in the wastewater. The DO concentration usually tends to be higher in the upper region and comparatively lower in the lower region across an up-flow CW-MFC [12]. At the anodic region, a higher rate of oxidation of pollutants facilitates more electron transfer to the cathodic region, which in turn speeds up the rate of reduction reactions at the cathode. This accelerates oxygen diffusion at the cathode, resulting in higher DO concentrations at the cathode. It was also observed that DO levels were slightly higher in CW-MFC (GAC) as compared to CW-MFC (GG), which indicates more COD removal in CW-MFC (GAC). The DO concentration at the lower anode decreased when organic loading was increased for both electrode materials because oxygen was consumed in the degradation of the organic substrate. The pH profile is also considered an important operative variable due to the possible effect of pH variation on electroactive bacteria [12]. The pH was found to be in the range of 4.2–6 for both of the microcosms during the course of the experiment. The pH was found to be decreased as the organic loading rate increased.

3.2. Chemical Oxygen Demand (COD) Removal Efficiency

Electrodes play a very crucial role in the degradation of pollutants. The degradation of pollutants depends on the composition, richness, and diversity of the microbial community, for which the selection of a suitable electrode becomes vital. The COD removal efficiency of CW-MFC (GG) and CW-MFC (GAC) for both organic loading rates is shown in Figure 3a,b. The overall average COD removal efficiency was observed at 70.44 ± 2% for CW-MFC (GG) at an organic loading rate of 890.11 g COD/m^3-d, wherein A1, A2, A3, and A4 achieved COD treatment contributions (from the initial loads) of 24.48 ± 2.3%,

28.10 ± 2.08%, 38.14 ± 4.45%, and 47.69 ± 1.2% respectively. Whereas, at the same organic loading rate, the overall average COD removal efficiency for CW-MFC (GAC) was observed at 95.24 ± 3.8% with individual anodes A1, A2, A3, and A4 exhibiting their contributions in removal at 53.68 ± 1.5%, 77.46 ± 1.8%, 81.23 ± 2.5%, and 86.02 ± 5%, respectively, as shown in Figure 3a. As depicted in Figure 3b, when the organic loading rate was increased from 890.11 g COD/m^3-d to 1781.32 g COD/m^3-d, the COD removal efficiency was decreased for both CW-MFCs. At a high organic loading rate, the average overall COD removal efficiency was observed to be 65.43 ± 2.4% and 88.16 ± 1.7%, respectively, for CW-MFC (GG) and CW-MFC (GAC). At A1, 22.14 ± 1.05% and 46.81 ± 1.5% of COD removal efficiency were observed for CW-MFC (GG) and CW-MFC (GAC), respectively. In CW-MFC (GG), treatment efficiencies of 26.61 ± 1.8%, 33.37 ± 2.2%, and 46.95 ± 1.7% observed at A2, A3, and A4, respectively. Likewise, the COD removal efficiency increased from 46.81 ± 1.5% to 65.28 ± 5.8% at A2, then gradually increased up to 69.36 ± 3.6% and 75.68 ± 4.9% at A3 and A4 in CW-MFC (GAC).

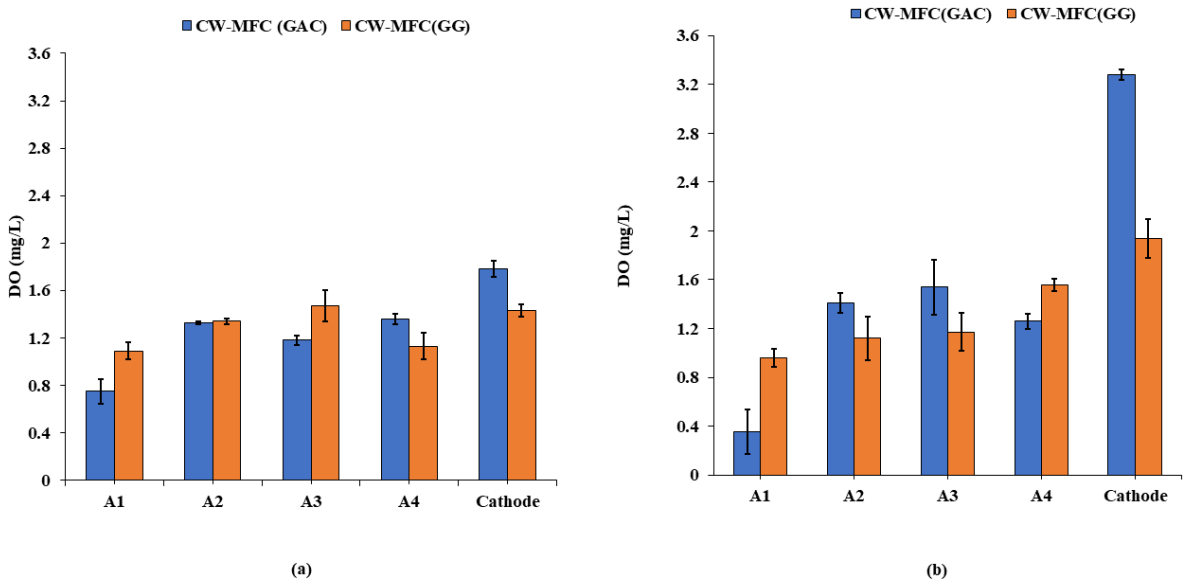

Figure 2. Dissolved oxygen (DO) profiles (**a**) at an organic loading rate of 890.11 g COD/m^3-d and (**b**) at an organic loading rate of 1781.32 g COD/m^3-d.

As observed from Figure 3a,b, CW-MFC (GAC) showed up to 86.02% and 75.68% treatment in the anodic zone for an organic loading rate of 890.11 g COD/m^3-d and 1781.32 g COD/m^3-d, respectively. On the other hand, in CW-MFC (GG), COD reduction was found to be less than 50% in the anodic zone for both organic loading rates. It shows that multi-anode CW-MFC works efficiently with granular activated charcoal electrode material under both organic loads. For an organic loading rate of 890.11 g COD/m^3-d, the treatment efficiency was found to be 24.8% higher in CW-MFC (GAC) than CW-MFC (GG), whereas it was 22.73% higher in CW-MFC (GAC) when the organic loading rate was increased to 1781.32 g COD/m^3-d. The reason for the comparatively better performance of CW-MFC (GAC) may be ascribed to the physical, chemical, and biological characteristics of the activated carbon. The activated charcoal retains properties like good electrical conductivity, lower resistivity, strong biocompatibility, porous architecture, a good electron transfer rate, better microbial adhesivity, significant chemical and mechanical stabilities, anti-corrosiveness, and large surface area [12]. This allows higher specific surface area and comparatively better environment for bacterial attachment. Moreover, the activated charcoal used in the study was saturated before conducting the study, thus eliminating the chances of adsorption-type mechanisms. Srivastava et al. [17] reported that overall COD removal was almost 6% higher in activated charcoal electrodes than in graphite electrodes in closed and open circuits for all studied organic loads. Li et al. [14] reported nearly

100% removal of SMZ using GAC electrodes, whereas it was less in the case of graphite electrodes.

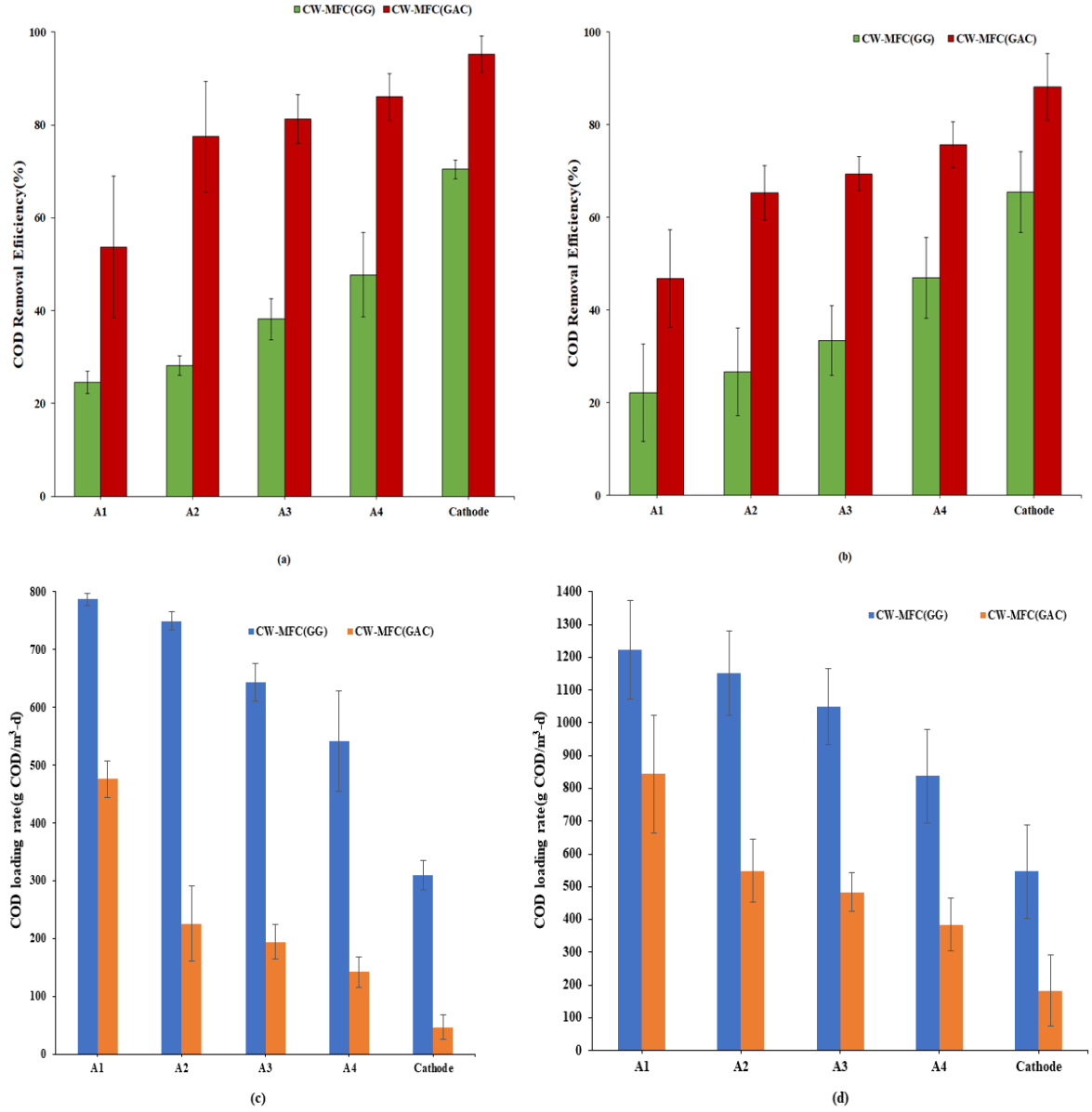

Figure 3. COD Removal efficiency (%) at an (**a**) organic loading rate of 890.11 g COD/m^3-d and (**b**) organic loading rate of 1781.32 g COD/m^3-d, (**c**,**d**) show COD loading rates from A1 to Cathode for an organic loading rate of 890.11 g COD/m^3-d and 1781.32 g COD/m^3-d, respectively.

Furthermore, in each case, the highest removal is observed at A1, which may be because of the high food-to-microbe ratio in the first portion of the studied system. At A1, bacteria might tend to convert water-soluble chemical substances, including hydrolysis products, to short-chain organic acids like formic, acetic, propionic, butyric, and pentanoic [31]. The unutilized organic matter transfers from A1 to A2, where it further gets degraded. A similar process repeats with A3 and A4 before it reaches the cathode. Generally, in CW-MFCs, microorganisms donate electrons to the anode electrode, which passes them to the cathode through a circuit where they react with oxidants (like oxygen) and protons. Consequently, due to the flow of electrons through the electrical circuit, electricity is generated. During this process, organic molecules first break down into simpler

intermediate molecules. The degradation of organic substrates can be explained by the anode (Equation (2)) and cathode reactions (Equation (3)).

$$C_6H_{12}O_6 \text{ (Glucose)} + 6H_2O \rightarrow 6CO_2 + 24H^+ + 24e^- \quad (2)$$

$$4H^+ + 4e^- + 2O_2 \rightarrow 2H_2O \quad (3)$$

In the present study, as it is clear from Figure 3a, at A1, the highest removal was achieved in both CW-MFC (GG) and CW-MFC (GAC). However, CW-MFC (GAC) removed 29.2% more COD than CW-MFC (GG) for an organic loading rate of 890.11 g COD/m^3-d. Similarly, at an organic loading rate of 1781.32 g COD/m^3-d also, 24.67% more treatment was observed in CW-MFC (GAC) than CW-MFC (GG) in A1.

It is also clear from the results that when the organic loading rate was increased, COD removal was decreased for both CW-MFCs. This is because more organic material is oxidized at a lower organic loading rate. A study by Villasenor et al. [32] also reported that organic material was completely oxidized at 13.9 gm COD/m^2-d, whereas it decreased by 5% when the organic loading rate was increased to 31.1 gm COD/m^2-d. Other researchers also reported better performance of CW-MFC under low organic conditions [23,33]. Conversely, some other researchers reported an improved treatment and power performance with increasing organic concentrations [12,34]. Yadav et al. [4] reported that high contaminant concentrations lead to slight acidification, which lowers the rate of degradation. Liu et al. [23] reported a decrease in COD removal efficiency from 95% to 81–90% and 81–85% when influent COD was increased gradually from 50 mg/L to 500 mg/L and finally 1000 mg/L. However, in the present study, despite the significant increase in organic loading, the removal efficiency was not much impacted due to the enhanced electrode surface area in multiple anode systems, even at such relatively higher organic loading rates.

Additionally, Figure 3c,d were also drawn to show COD loading rates starting from A1 to the cathode in CW-MFC(GG) and CW-MFC(GAC) to represent degradation of organics at each stage for an organic loading rate of 890.11 g COD/m^3-d and 1781.32 g COD/m^3-d during the course of the experiment. It is clearly evident from Figure 3a–d that the COD loading rate is consistently decreasing as the wastewater passes from A1 to cathode for both organic loading rates.

From the overall COD results for CW-MFC (GG) and CW-MFC (GAC) under both organic loading rates, three distinct points can be concluded: (i) treatment efficiency decreases as the organic loading rate increases; (ii) highest removal efficiency is achieved at A1; and (iii) GAC performed better than GG. It is also noted that multiple anode systems provided a comparatively larger anodic portion to facilitate the oxidation reactions taking place at the anode, which was reflected in COD removal efficiency, that decreased only about 5% in the case of CW-MFC (GG) and about 7% in the case of CW-MFC (GAC) even after doubling the glucose load. This indicates an enhancement in the anode potential due to the multiple electrode systems, which can treat significantly higher organic loads.

3.3. Ammonium Removal

Ammonium removal is a challenge in the traditional constructed wetland as it demands the availability of electron acceptors during the nitrification step involving the conversion of ammonium to nitrate (or nitrite) by the *Nitrosomonas* and *Nitrobacter* microbial communities. However, traditional CWs are dominated by anaerobic regions, indicating the unavailability or low availability of electron acceptors, thus challenging ammonium removal [35,36]. Figure 4 shows the percentage removal of ammonium (NH_4^+-N) obtained in the present study. The ammonium (NH_4^+-N) concentration was measured from the influent and effluent at both organic loading rates. The NH_4^+-N removal efficiency in CW-MFC (GG) was obtained as 56.29 ± 7% and 56.09 ± 3.9% for the organic loading rates of 890.11 g COD/m^3-d and 1781.32 g COD/m^3-d, respectively. Whereas, in the case of CW-MFC(GAC), 36.59 ± 3.8% and 50.59 ± 7% NH_4^+-N removal were observed at an organic loading rate of 890.11 g COD/m^3-d and 1781.32 g COD/m^3-d, respectively.

CW-MFC (GG) exhibited higher ammonium removal at both organic loads in comparison to CW-MFC (GAC). However, DO concentration at both organic loads in CW-MFC (GG) was considerably low, lying in the range of 0.75 ± 0.06–1.94 ± 0.07 mg/L, suggesting anaerobic conditions throughout the system and thus indicating the negligible role of DO towards ammonium removal. Similar DO concentrations are also observed in other CW-MFC studies using granular graphite as a conductive material [36]. High ammonium removal in DO-deficient environments can be explained by the presence of conductive granular graphite as an electrode material. The conductive materials can function as solid electron acceptors in the anaerobic region, facilitating ammonium removal. Our results are in accordance with the results presented by Srivastava et al. [36], who concluded that the electrode-dependent ammonium oxidation process is the reason for the high removal of ammonium in CW-MFC.

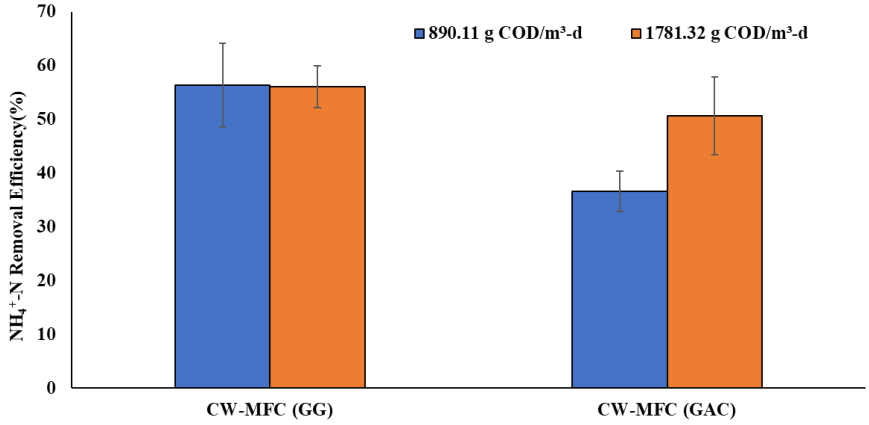

Figure 4. NH_4^+-N removal efficiency at an organic loading rate of 890.11 g COD/m^3-d and 1781.32 g COD/m^3-d.

Furthermore, in the case of CW-MFC (GAC), higher ammonium removal can be observed with an increase in load. However, the increase in load from 890.11 g COD/m^3-d to 1781.32 g COD/m^3-d has decreased the DO availability from 0.75 mg/L to 0.35 mg/L in CW-MFC (GAC). This decrease in DO levels will increase the competitiveness between nitrifiers and heterotrophs for available oxygen, which could limit ammonium removal with an increase in organic load [37]. Further study is needed to explain such results. Although this indicates the crucial role of conductive material and the possible efficiency of electron conductivity as a deciding factor in ammonium removal even at high organic loading rates. Furthermore, the implementation of multiple anodes has increased the electrode surface area and enhanced attachment sites for microbes, which is further responsible for high ammonium removal efficiency. CW-MFC (GAC) has shown an increase in ammonium removal with an increase in organic loading rate, while it is consistent in the case of CW-MFC (GG). This may be due to the increase in DO level in the cathodic region of CW-MFC (GAC) during that phase because of some unforeseen/unexplainable reasons, as shown in Figure 2. As depicted in Figure 4, under both organic loading rates, CW-MFC (GG) showed better NH_4^+-N removal than CW-MFC (GAC). This may be explained by the fact that graphite acted as a better electron acceptor than charcoal to accept the electrons released in the process of NH_4^+-N oxidation.

3.4. Electricity Generation

The voltage profiles of CW-MFC (GG) and CW-MFC (GAC) throughout the experiment are presented in Table 1. The maximum voltage was recorded with the uppermost anode electrode i.e., A4 and cathode (A4-C) for both the microcosms as 47.9 mV for CW-MFC (GG) and 139.9 mV for CW-MFC (GAC). The lowest voltage was achieved between the bottom most anode electrode and cathode i.e., A1-C for both CW-MFC (GG) and CW-MFC (GAC) as 30.1 mV and 13.6 mV at an organic loading rate of 890.11 g COD/m^3-d and 30 mV

and 13.2 mV at an organic loading rate of 1781.32 g COD/m^3-d, respectively, as shown in Table 1. This may be due to the lowest spacing between A4 and the cathode, whereas spacing is highest in the case of A1 and the cathode. Lower electrode distance enhances the voltage output by decreasing the internal resistance in CW-MFC (GG) and CW-MFC (GAC) systems [38–41]. The spacing between the electrodes plays an important role in electricity production [7,19,42].

Table 1. Showing maximum voltage (V_{max}), power density (Pd_{max}), and current density (Cd_{max}) under both organic loading rates.

	CW-MFC(GG)						**CW-MFC(GAC)**					
Organic Loading Rate	**890.11 g COD/m^3-d**			**1781.32 g COD/m^3-d**			**890.11 g COD/m^3-d**			**1781.32 g COD/m^3-d**		
Connections	**Pd_{max}** (mW/m^3)	**Cd_{max}** (mA/m^3)	**V_{max}** (mV)	**Pd_{max}** (mW/m^3)	**Cd_{max}** (mA/m^3)	**V_{max}** (mV)	**Pd_{max}** (mW/m^3)	**Cd_{max}** (mA/m^3)	**V_{max}** (mV)	**Pd_{max}** (mW/m^3)	**Cd_{max}** (mA/m^3)	**V_{max}** (mV)
A1-C	2.26	75.25	30.1	2.25	75	30	0.462	36.75	13.6	0.43	35.67	13.2
A2-C	1.69	65	26.4	2.13	73	29.2	1.42	64.59	23.9	4.47	114.32	42.3
A3-C	3.80	97.5	39.5	2.73	82.75	33.1	17.80	228.10	84.4	16.76	221.35	81.9
A4-C	5.52	117.5	47.9	4.36	104.5	41.8	48.30	375.67	139.9	30.25	297.3	110.6

Furthermore, results suggested a decrease in voltage generation with an increase in organic loading rate from 890.11 g COD/m^3-d to 1781.32 g COD/m^3-d for both microcosms. In the case of CW-MFC (GG), voltage decreased from 47.9 mV to 41.8 mV, whereas for CW-MFC (GAC), it decreased from 139.9 mV to 110.6 mV with an increase in organic load from 890.11 g COD/m^3-d to 1781.32 g COD/m^3-d, respectively, for A4-C, as shown in Table 1. This may be due to the prevalence of methanogenic microorganisms over exo-electrogenic biofilms as high organic loading tends to promote the growth of methanogenic bacteria. A lower organic loading rate, on the other hand, benefits the growth of exo-electrogenic bacteria and activity over competing for methanogenesis [7]. Another reason for lower electrical output can be that when OLR increases, the electrons get neutralized in the anodic chamber itself by other electron acceptors such as nitrate, sulfate, chlorinated compounds, etc., already present in the wastewater [43]. Other studies also reported that when influent COD concentrations are very high, non-oxidized organic matter moves from the anodic region to the cathode, allowing a lack of proton exchange and dissolved oxygen in the cathode. Thus, this low DO in the bio-cathode surface results in lower power output [23].

It is also observed that the voltage achieved at both organic loads is low. The power output in the present study was comparatively lower than other multi-anode studies reported in the literature [24,25]. This may be due to high organic loading and a lack of artificial aeration in the cathodic zone. It indicates the involvement of electrons released during the oxidation of organic material in other reactions, such as methanogenesis, instead of contributing towards electricity generation [36]. The low voltages obtained at both OLR can also be correlated with the slightly acidic pH recorded throughout the course of the experiment. In a multi-anode setup, Oon et al. [38] recorded average voltages of 286 ± 13 mV and 421 ± 16 mv at 314 mg/L and 624 mg/L organic loadings, which are lower than the organic loads in the present study.

The voltage output of CW-MFC (GAC) was found to be better than CW-MFC (GG) under both organic loads. This can be due to the higher specific surface area of granular activated carbon compared to granular graphite, which would have provided a better attachment site to exo-electrogenic biofilm [16,44,45]. Similarly, the power output of CW-MFC having charcoal electrodes was reported to be better than CW-MFC having graphite electrodes in a study conducted by another researcher [17]. The study reported a maximum power density of 43.63 mW/m^3 for GAC as anode and cathode electrode material and 0.10 mW/m^3 for GG as anode and cathode electrode material.

Furthermore, current density and power density were calculated at each anode at different loading rates to plot the polarization curves. Table 1 shows the variation of current

and power density with organic loading rate for both microcosms. Results indicate a decrease in both current and power density with an increase in load in the case of both CW-MFC (GG) and CW-MFC (GAC). This could result from a decrease in electrogenic microbial activity and increased methanogenic activity and or inhibition of the microbial activity at higher loads. Further, Figure 5a–d show the polarization curves of each anode at both loading rates. The maximum current density and power density were observed for A4-C of 117.5 mA/m^3, 5.52 mW/m^3 for CW-MFC (GG), and 375.67 mA/m^3, 48.30 mW/m^3 for CW-MFC (GAC) at an OLR of 890.11 g COD/m^3-d. Whereas, with an increase in OLR to 1781.32 g COD/m^3-d, maximum current density and power density produced at A4-C were observed as 104.5 mA/m^3, 4.36 mW/m^3, and 297.3 mA/m^3; 30.25 mW/m^3 for CW-MFC (GG) and CW-MFC (GAC), respectively. This indicates that CW-MFC (GAC) produced more current and power density at both organic loading rates, as also presented in Table 1. The distance between electrodes is a crucial factor for the electrical performance of CW-MFC [24]. In the present study, the distance between the anode and cathode was lowest in the case of A4, whereas it was highest in the case of A1. This may be the reason for the comparatively better power output at A4-C. Oon et al. [29] also reported the lowest power density for the anode placed at the farthest distance from the cathode. It is well reported in the literature that as the distance between electrodes increases, the internal resistance also increases, which in turn lowers the power output of CW-MFC [40,46,47]. It is also evident from Table 1 that power output decreased when the organic loading rate was increased. Bolton and Randall [48] also reported a 44% decrease in power output when COD was increased. This may be due to the dominance of the methanogenic environment, which led to the utilization of only a small fraction of substrate into electrical output. Furthermore, a gradual decrease in power density was also observed by Xu et al. [28], when the OLR was raised above 18.4 g COD/m^2/d. Another reason for the decrease in power and current densities with OLR is that the undegraded substrate from the anode moves to the cathode and produces anaerobic conditions, thus hindering cathodic reactions [49].

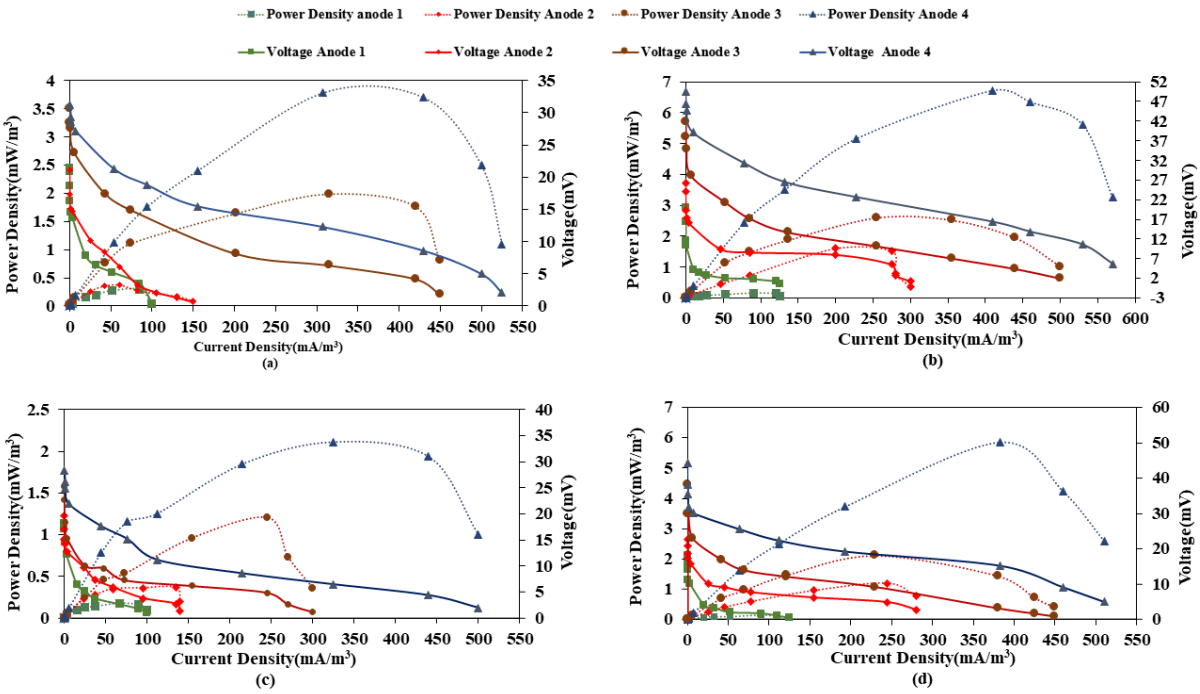

Figure 5. Polarization curves for (**a**) CW-MFC (GG), (**b**) CW-MFC(GAC) at an organic loading rate of 890.11 g COD/m^3-d, (**c**) CW-MFC (GG), and (**d**) CW-MFC (GAC) at an organic loading rate of 1781.32 g COD/m^3-d.

4. Conclusions

The present study investigated the potential of multi-anode and single-cathode CW-MFCs for treating significantly higher OLRs. The study concludes that even with the doubling of the OLRs from 890.11 g COD/m^3-d to 1781.32 g COD/m^3-d, there is an insignificant change in COD removal efficiency, as it decreased only about 5% in the case of CW-MFC (GG) and about 7% in the case of CW-MFC (GAC) with the increase in OLRs. This signifies that the multiple anode system provided a larger anodic portion to facilitate the oxidation reactions taking place at the anode. Significant ammonium removal was observed at even such high OLRs, which was attributed to the increase in electrode surface area and enhanced attachment sites for microbes with the implementation of multiple anodes. Moreover, conductive materials have also played a crucial role in ammonium removal at high OLRs by functioning as electron acceptors released during the process of NH_4^+-N oxidation, and thus CW-MFC (GG) outperformed CW-MFC (GAC) due to the higher electron acceptor tendency of GG over GAC. A maximum power density of 43.63 mW/m^3 was observed for GAC at anode and cathode electrode materials resulting from the high specific surface area of GAC compared to GG, which provided a better attachment site to exo-electrogenic biofilm. Decisively, a multi-anode CW-MFC configuration with GAC and GG as electrode materials has substantial potential to treat considerably high OLR and can be investigated further for real wastewater containing high OLR.

Supplementary Materials: The following supporting information can be downloaded at: https://www.mdpi.com/article/10.3390/en16020784/s1.

Author Contributions: Conceptualization, A.K.Y. and P.T.; methodology, A.K.Y. and P.T.; software, P.T.; validation, P.T., Y.M., A.K.Y. and N.R.; formal analysis, P.T.; investigation, P.T.; resources, A.K.Y.; data curation, P.T., Y.M., A.K.Y. and N.R.; writing—original draft preparation, P.T. and Y.M.; writing—P.T., Y.M., A.K.Y. and N.R.; visualization, P.T., Y.M., A.K.Y. and N.R.; supervision, A.K.Y. and N.R.; project administration, A.K.Y. and N.R.; funding acquisition, A.K.Y. and N.R. All authors have read and agreed to the published version of the manuscript.

Funding: P.T. acknowledges the funding provided by UGC NET-JRF. A.K.Y. acknowledge yhe grant under TMD Scheme (DST, New Delhi) [DST/TMD-EWO/WTI/2K19/EWFH/2019/109 (G2)]. NR are acknowledges the funding provided by Guru Gobind Singh Indraprastha University, Delhi, India under Faculty Research Grant Scheme (F. No. GGSIPU/DRC/FRGS/2018/40(1115)[2]).

Institutional Review Board Statement: Not applicable.

Informed Consent Statement: Not applicable.

Data Availability Statement: Authors do not have permission to share the data.

Conflicts of Interest: The authors declare no conflict of interest.

References

1. Gupta, S.; Mittal, Y.; Panja, R.; Prajapati, K.B.; Yadav, A.K. Conventional Wastewater Treatment Technologies. *Curr. Dev. Biotechnol. Bioeng.* **2021**, *35*, 47–75.
2. Srivastava, P.; Gupta, S.; Mittal, Y.; Dhal, N.K.; Saeed, T.; Martínez, F.; Yadav, A.K. Constructed Wetlands and Its Coupling with Other Technologies from Lab to Field Scale for Enhanced Wastewater Treatment and Resource Recovery. In *Novel Approaches towards Wastewater Treatment and Resource Recovery Technologies*; Elsevier: Amsterdam, The Netherlands, 2022; pp. 419–446.
3. Doherty, L.; Zhao, Y.; Zhao, X.; Hu, Y.; Hao, X.; Xu, L.; Liu, R. A Review of a Recently Emerged Technology: Constructed Wetland–Microbial Fuel Cells. *Water Res.* **2015**, *85*, 38–45. [CrossRef] [PubMed]
4. Yadav, A.K.; Dash, P.; Mohanty, A.; Abbassi, R.; Mishra, B.K. Performance Assessment of Innovative Constructed Wetland-Microbial Fuel Cell for Electricity Production and Dye Removal. *Ecol. Eng.* **2012**, *47*, 126–131. [CrossRef]
5. Srivastava, P.; Dwivedi, S.; Kumar, N.; Abbassi, R.; Garaniya, V.; Yadav, A.K. Performance Assessment of Aeration and Radial Oxygen Loss Assisted Cathode Based Integrated Constructed Wetland-Microbial Fuel Cell Systems. *Bioresour. Technol.* **2017**, *244*, 1178–1182. [CrossRef] [PubMed]
6. Srivastava, P.; Abbassi, R.; Yadav, A.K.; Garaniya, V.; Lewis, T.; Zhao, Y.; Aminabhavi, T. Interrelation between Sulphur and Conductive Materials and Its Impact on Ammonium and Organic Pollutants Removal in Electroactive Wetlands. *J. Hazard. Mater.* **2021**, *419*, 126417. [CrossRef]

7. Huang, X.; Duan, C.; Duan, W.; Sun, F.; Cui, H.; Zhang, S.; Chen, X. Role of Electrode Materials on Performance and Microbial Characteristics in the Constructed Wetland Coupled Microbial Fuel Cell (CW-MFC): A Review. *J. Clean. Prod.* **2021**, *301*, 126951. [CrossRef]
8. Tamta, P.; Rani, N.; Yadav, A.K. Enhanced Wastewater Treatment and Electricity Generation Using Stacked Constructed Wetland–Microbial Fuel Cells. *Environ. Chem. Lett.* **2020**, *18*, 871–879. [CrossRef]
9. Gupta, S.; Srivastava, P.; Patil, S.A.; Yadav, A.K. A Comprehensive Review on Emerging Constructed Wetland Coupled Microbial Fuel Cell Technology: Potential Applications and Challenges. *Bioresour. Technol.* **2021**, *320*, 124376. [CrossRef]
10. Srivastava, P.; Gupta, S.; Garaniya, V.; Abbassi, R.; Yadav, A.K. Up to 399 MV Bioelectricity Generated by a Rice Paddy-Planted Microbial Fuel Cell Assisted with a Blue-Green Algal Cathode. *Environ. Chem. Lett.* **2019**, *17*, 1045–1051. [CrossRef]
11. Srivastava, P.; Abbassi, R.; Yadav, A.; Garaniya, V.; Asadnia, M.; Lewis, T.; Khan, S.J. Influence of Applied Potential on Treatment Performance and Clogging Behaviour of Hybrid Constructed Wetland-Microbial Electrochemical Technologies. *Chemosphere* **2021**, *284*, 131296. [CrossRef]
12. Ebrahimi, A.; Sivakumar, M.; McLauchlan, C. A Taxonomy of Design Factors in Constructed Wetland-Microbial Fuel Cell Performance: A Review. *J. Environ. Manag.* **2021**, *291*, 112723. [CrossRef] [PubMed]
13. Guo, K.; Donose, B.C.; Soeriyadi, A.H.; Prévoteau, A.; Patil, S.A.; Freguia, S.; Gooding, J.J.; Rabaey, K. Flame Oxidation of Stainless Steel Felt Enhances Anodic Biofilm Formation and Current Output in Bioelectrochemical Systems. *Environ. Sci. Technol.* **2014**, *48*, 7151–7156. [CrossRef] [PubMed]
14. Li, H.; Song, H.-L.; Yang, X.-L.; Zhang, S.; Yang, Y.-L.; Zhang, L.-M.; Xu, H.; Wang, Y.-W. A Continuous Flow MFC-CW Coupled with a Biofilm Electrode Reactor to Simultaneously Attenuate Sulfamethoxazole and Its Corresponding Resistance Genes. *Sci. Total Environ.* **2018**, *637*, 295–305. [CrossRef] [PubMed]
15. Mittal, Y.; Srivastava, P.; Kumar, N.; Kumar, M.; Singh, S.K.; Martinez, F.; Yadav, A.K. Ultra-Fast and Low-Cost Electroactive Biochar Production for Electroactive-Constructed Wetland Applications: A Circular Concept for Plant Biomass Utilization. *Chem. Eng. J.* **2023**, *452*, 138587. [CrossRef]
16. Taskan, E.; Hasar, H. Comprehensive Comparison of a New Tin-Coated Copper Mesh and a Graphite Plate Electrode as an Anode Material in Microbial Fuel Cell. *Appl. Biochem. Biotechnol.* **2015**, *175*, 2300–2308. [CrossRef]
17. Srivastava, P.; Yadav, A.K.; Mishra, B.K. The Effects of Microbial Fuel Cell Integration into Constructed Wetland on the Performance of Constructed Wetland. *Bioresour. Technol.* **2015**, *195*, 223–230. [CrossRef]
18. Zhang, H.; Zhang, R.; Zhang, G.; Yang, F.; Gao, F. Modified Graphite Electrode by Polyaniline/Tourmaline Improves the Performance of Bio-Cathode Microbial Fuel Cell. *Int. J. Hydrog. Energy* **2014**, *39*, 11250–11257. [CrossRef]
19. Kim, C.; Kim, J.R.; Heo, J. Enhancement of Bioelectricity Generation by a Microbial Fuel Cell Using Ti Nanoparticle-modified Carbon Electrode. *J. Chem. Technol. Biotechnol.* **2019**, *94*, 1622–1627. [CrossRef]
20. Wang, J.; Song, X.; Li, Q.; Bai, H.; Zhu, C.; Weng, B.; Yan, D.; Bai, J. Bioenergy Generation and Degradation Pathway of Phenanthrene and Anthracene in a Constructed Wetland-Microbial Fuel Cell with an Anode Amended with NZVI. *Water Res.* **2019**, *150*, 340–348. [CrossRef]
21. Santoro, C.; Artyushkova, K.; Babanova, S.; Atanassov, P.; Ieropoulos, I.; Grattieri, M.; Cristiani, P.; Trasatti, S.; Li, B.; Schuler, A.J. Parameters Characterization and Optimization of Activated Carbon (AC) Cathodes for Microbial Fuel Cell Application. *Bioresour. Technol.* **2014**, *163*, 54–63. [CrossRef]
22. Estrada-Arriaga, E.B.; Guadarrama-Pérez, O.; Silva-Martínez, S.; Cuevas-Arteaga, C.; Guadarrama-Pérez, V.H. Oxygen Reduction Reaction (ORR) Electrocatalysts in Constructed Wetland-Microbial Fuel Cells: Effect of Different Carbon-Based Catalyst Biocathode during Bioelectricity Production. *Electrochim. Acta* **2021**, *370*, 137745. [CrossRef]
23. Liu, S.; Song, H.; Wei, S.; Yang, F.; Li, X. Bio-Cathode Materials Evaluation and Configuration Optimization for Power Output of Vertical Subsurface Flow Constructed Wetland—Microbial Fuel Cell Systems. *Bioresour. Technol.* **2014**, *166*, 575–583. [CrossRef] [PubMed]
24. Tang, C.; Zhao, Y.; Kang, C.; Yang, Y.; Morgan, D.; Xu, L. Towards Concurrent Pollutants Removal and High Energy Harvesting in a Pilot-Scale CW-MFC: Insight into the Cathode Conditions and Electrodes Connection. *Chem. Eng. J.* **2019**, *373*, 150–160. [CrossRef]
25. Oon, Y.-L.; Ong, S.-A.; Ho, L.-N.; Wong, Y.-S.; Dahalan, F.A.; Oon, Y.-S.; Lehl, H.K.; Thung, W.-E. Synergistic Effect of Up-Flow Constructed Wetland and Microbial Fuel Cell for Simultaneous Wastewater Treatment and Energy Recovery. *Bioresour. Technol.* **2016**, *203*, 190–197. [CrossRef] [PubMed]
26. Wang, L.; Pang, Q.; Zhou, Y.; Peng, F.; He, F.; Li, W.; Xu, B.; Cui, Y.; Zhu, X. Robust Nitrate Removal and Bioenergy Generation with Elucidating Functional Microorganisms under Carbon Constraint in a Novel Multianode Tidal Constructed Wetland Coupled with Microbial Fuel Cell. *Bioresour. Technol.* **2020**, *314*, 123744. [CrossRef]
27. Yang, Y.; Zhao, Y.; Tang, C.; Liu, R.; Chen, T. Dual Role of Macrophytes in Constructed Wetland-Microbial Fuel Cells Using Pyrrhotite as Cathode Material: A Comparative Assessment. *Chemosphere* **2021**, *263*, 128354. [CrossRef]
28. Xu, L.; Zhao, Y.; Wang, X.; Yu, W. Applying Multiple Bio-Cathodes in Constructed Wetland-Microbial Fuel Cell for Promoting Energy Production and Bioelectrical Derived Nitrification-Denitrification Process. *Chem. Eng. J.* **2018**, *344*, 105–113. [CrossRef]
29. Oon, Y.-L.; Ong, S.-A.; Ho, L.-N.; Wong, Y.-S.; Oon, Y.-S.; Lehl, H.K.; Thung, W.-E. Hybrid System Up-Flow Constructed Wetland Integrated with Microbial Fuel Cell for Simultaneous Wastewater Treatment and Electricity Generation. *Bioresour. Technol.* **2015**, *186*, 270–275. [CrossRef]

30. Logan, B.E.; Hamelers, B.; Rozendal, R.; Schröder, U.; Keller, J.; Freguia, S.; Aelterman, P.; Verstraete, W.; Rabaey, K. Microbial Fuel Cells: Methodology and Technology. *Environ. Sci. Technol.* **2006**, *40*, 5181–5192. [CrossRef]
31. Chakrabarti, S.; Roychoudhury, P.; Bajpai, P. Biphasic Biomethanation of Wood-Hydrolysate Effluent. *Artif. Cells Blood Substit. Biotechnol.* **1999**, *27*, 461–467. [CrossRef]
32. Villasenor, J.; Capilla, P.; Rodrigo, M.; Canizares, P.; Fernandez, F. Operation of a Horizontal Subsurface Flow Constructed Wetland–Microbial Fuel Cell Treating Wastewater under Different Organic Loading Rates. *Water Res.* **2013**, *47*, 6731–6738. [CrossRef] [PubMed]
33. Wang, J.; Song, X.; Wang, Y.; Zhao, Z.; Wang, B.; Yan, D. Effects of Electrode Material and Substrate Concentration on the Bioenergy Output and Wastewater Treatment in Air-Cathode Microbial Fuel Cell Integrating with Constructed Wetland. *Ecol. Eng.* **2017**, *99*, 191–198. [CrossRef]
34. Wu, D.; Yang, L.; Gan, L.; Chen, Q.; Li, L.; Chen, X.; Wang, X.; Guo, L.; Miao, A. Potential of Novel Wastewater Treatment System Featuring Microbial Fuel Cell to Generate Electricity and Remove Pollutants. *Ecol. Eng.* **2015**, *84*, 624–631. [CrossRef]
35. Ghangrekar, M.; Shinde, V. Performance of Membrane-Less Microbial Fuel Cell Treating Wastewater and Effect of Electrode Distance and Area on Electricity Production. *Bioresour. Technol.* **2007**, *98*, 2879–2885. [CrossRef]
36. Srivastava, P.; Yadav, A.K.; Garaniya, V.; Lewis, T.; Abbassi, R.; Khan, S.J. Electrode Dependent Anaerobic Ammonium Oxidation in Microbial Fuel Cell Integrated Hybrid Constructed Wetlands: A New Process. *Sci. Total Environ.* **2020**, *698*, 134248. [CrossRef]
37. Riley, K.A.; Stein, O.R.; Hook, P.B. Ammonium Removal in Constructed Wetland Microcosms as Influenced by Season and Organic Carbon Load. *J. Environ. Sci. Health* **2005**, *40*, 1109–1121. [CrossRef]
38. Mittal, Y.; Dash, S.; Srivastava, P.; Mishra, P.M.; Aminabhavi, T.M.; Yadav, A.K. Azo Dye Containing Wastewater Treatment in Earthen Membrane Based Unplanted Two Chambered Constructed Wetlands-Microbial Fuel Cells: A New Design for Enhanced Performance. *Chem. Eng. J.* **2022**, *427*, 131856. [CrossRef]
39. Saket, P.; Mittal, Y.; Bala, K.; Joshi, A.; Kumar Yadav, A. Innovative Constructed Wetland Coupled with Microbial Fuel Cell for Enhancing Diazo Dye Degradation with Simultaneous Electricity Generation. *Bioresour. Technol.* **2022**, *345*, 126490. [CrossRef]
40. Xie, T.; Jing, Z.; Hu, J.; Yuan, P.; Liu, Y.; Cao, S. Degradation of Nitrobenzene-Containing Wastewater by a Microbial-Fuel-Cell-Coupled Constructed Wetland. *Ecol. Eng.* **2018**, *112*, 65–71. [CrossRef]
41. Yadav, A.K.; Mittal, Y.; Basu, S.; Kumar, T.P.; Srivastava, P.; Gupta, S. *Earthen Membrane Based Two Chambered Constructed Wetland Cum Micriobial Fuel Cell for Treatment and Detoxification of Waste Water Containing Azo Dye*; Wiley: Hoboken, NJ, USA, 2022.
42. Xu, L.; Zhao, Y.; Tang, C.; Doherty, L. Influence of Glass Wool as Separator on Bioelectricity Generation in a Constructed Wetland-Microbial Fuel Cell. *J. Environ. Manag.* **2018**, *207*, 116–123. [CrossRef]
43. Velvizhi, G.; Mohan, S.V. Electrogenic Activity and Electron Losses under Increasing Organic Load of Recalcitrant Pharmaceutical Wastewater. *Int. J. Hydrog. Energy* **2012**, *37*, 5969–5978. [CrossRef]
44. Sun, Y.; Wei, J.; Liang, P.; Huang, X. Electricity Generation and Microbial Community Changes in Microbial Fuel Cells Packed with Different Anodic Materials. *Bioresour. Technol.* **2011**, *102*, 10886–10891. [CrossRef]
45. Yang, Y.; Zhao, Y.; Tang, C.; Mao, Y.; Shen, C. Significance of Water Level in Affecting Cathode Potential in Electro-Wetland. *Bioresour. Technol.* **2019**, *285*, 121345. [CrossRef] [PubMed]
46. Oon, Y.-L.; Ong, S.-A.; Ho, L.-N.; Wong, Y.-S.; Dahalan, F.A.; Oon, Y.-S.; Lehl, H.K.; Thung, W.-E.; Nordin, N. Role of Macrophyte and Effect of Supplementary Aeration in Up-Flow Constructed Wetland-Microbial Fuel Cell for Simultaneous Wastewater Treatment and Energy Recovery. *Bioresour. Technol.* **2017**, *224*, 265–275. [CrossRef] [PubMed]
47. Liu, H.; Cheng, S.; Logan, B.E. Power Generation in Fed-Batch Microbial Fuel Cells as a Function of Ionic Strength, Temperature, and Reactor Configuration. *Environ. Sci. Technol.* **2005**, *39*, 5488–5493. [CrossRef]
48. Bolton, C.R.; Randall, D.G. Development of an Integrated Wetland Microbial Fuel Cell and Sand Filtration System for Greywater Treatment. *J. Environ. Chem. Eng.* **2019**, *7*, 103249. [CrossRef]
49. Wang, X.; Tian, Y.; Liu, H.; Zhao, X.; Wu, Q. Effects of Influent COD/TN Ratio on Nitrogen Removal in Integrated Constructed Wetland–Microbial Fuel Cell Systems. *Bioresour. Technol.* **2019**, *271*, 492–495. [CrossRef]